Published in the Slovak Republic
International Journal of Environmental Problems
Has been issued since 2015.
E-ISSN: 2413-7561
2020, 6(1): 11-24

DOI: 10.13187/ijep.2020.1.11
www.ejournal33.com


# Remote Sensing Application in Mapping Agricultural Crop Areas and Monitoring Rice Maturity

Nguyen Quoc Hiep [a, *], Nguyen Anh Hung [a], Pham Quang Loi [a], Pham Thi Thu Hien [a], Nguyen Duy Khanh [a]

[a] Center for Water Resources Software, VietNam Academy for Water Resources, Ministry of Agriculture and Rural Development, Vietnam

**Abstract**

Climate change has evolved in an unpredictable trend and droughts have occurred more and more severely in the central provinces of Vietnam. Determining the irrigated area and water requirement for various crops and the growth stage of each crop is an urgent need as water resources for irrigation are getting scarce year by year. This research examines the application of Sentinel-2 and Sentinel-1 images to map crop areas and identify the current development stage of paddy rice areas. The images are collected and pre-processed from 2017 to 2018 for Ha Tinh Province in Vietnam. The Maximus Likelihood method is used to interpret Sentinel-2 imagery for mapping agricultural crop distribution status. The research presents a new approach for identifying rice maturity using the Sentinel-1 image series. The Overall Accuracy (OA) and Kappa coefficient methods are used to evaluate the generated maps of the agricultural crop's distribution status. This study shows the relationship between the Sentinel-1 VH band and the growth of rice. From the image bands, we could calculate the slope of the line correlating between the VH backscattering value and the growth time of rice. Along with the local planting schedule, rice life cycle, and simple deduction, we could determine the rice growth stage at each time of image acquisition. The result will be the input parameter for the irrigation management, monitoring and operating information system that is applied to Ha Tinh province for proper and effective irrigation. The results identifying the rice maturity progression are illustrated for Cam Hoa commune in Cam Xuyen district and Thach Hoi commune in Thach Ha district, Ha Tinh Province.

**Keywords:** remote sensing, map of agricultural crop, rice maturity.

## 1. Introduction

In recent years, climate change has evolved in an unpredictable trend and droughts have occurred more and more severely in the central provinces of Vietnam. Determining the irrigated area and water requirement for various crops and the growth stage of each crop is an urgent need as water resources for irrigation are getting scarce year by year.

Various studies have used free satellite imagery to map crop classification. For example, a crop classification map for a province of Valencia (Spain) was obtained from the Sentinel-1 and Sentinel-2 data using the decision tree method with an accuracy of 93.96 % (Manuel et al., 2019); applying the Random Forest (RF) algorithm on Sentinel-2 and Landsat-8 data in semi-arid

[*] Corresponding author
E-mail addresses: nguyenquochiep@cwrs-au.vn (N. Quoc Hiep)

environments in the Eastern Mediterranean (Stavros Patsalidis et al., 2019); Using the Maximum Likelihood (MLC), Support Vector Machine (SVM), RF method to produce crop distribution maps from Sentinel-2, Landsat-8 (Raziye Hale et al., 2016; Neetu et al., 2019; Licheng Zhao et al., 2019; Tian-Xiang Zhang et al., 2019); Accurate classification for Land use and land cover maps using SVM algorithm on Sentinel-2 to analyze the data (Cavur et al., 2019; Immitzer et al., 2016).

Conventional optical images were affected by cloud cover and thus, the use of radar images to determine the growth stage of the rice has captured the attention of many researchers. For instance, using Monte Carlo simulation with RADARSAT data to predict rice maturity (Wang et al., 2005); Using ENVISAT/ASAR data to establish a rice map for the Mekong Delta in Vietnam, piloted in An Giang province with an overall accuracy of 85.3 % and the kappa coefficient of 0.74 (Bouvet et al., 2011; Nguyen et al., 2015) and a series of studies using radar satellite images to map rice distribution (Lopez-Sanchez et al., 2011; Nelson et al., 2014; Clauss et al., 2018; Lasko et al., 2018; Ndikumana et al., 2018). In addition, a group of authors used machine learning algorithms training Sentinel-1 data to identify the rice, its yield, and height. The study was conducted in the Camargue region, southern France. Height and biomass of rice were calculated based on Sentinel-1 data trained by machine learning algorithms, Multiple Linear Regression (MLR), Support Vector Regression (SVR) and RF. The results showed that the correlation between the polarization of VH Sentinel-1 and biomass is also very high with R2 = 0.9 and RMSE = 18 % (162 g·m-2) (with RF method) (Ndikumana et al., 2018). Using a combination of Gaussian distribution, VV/VH variance and slope coefficient of the linear regression equation of the VH series of Sentinel-1 imagery was performed for crop mapping. The overall accuracy obtained was 96.3 % by using the decision tree and 96.6 % by using the RF classification (Hassan Bazzi et al., 2019).

The above studies focused on rice mapping for the whole crop development. The algorithm for determining rice maturity is not feasible when applied on such large scales as a province or a country in a short period of time. This study focuses on the use of Sentinel-2 imagery data to map agricultural crop areas and the use of Sentinel-1 image series data to determine the current growth stage of rice cultivation areas. A new approach for determining rice maturity using the Sentinel-1 SAR series in Ha Tinh province, Vietnam is proposed. Identified rice and other crop cultivation areas and its growth stages at a certain period is a useful source of information to improve irrigation efficiency in Ha Tinh province. The paper is structured in the following main sections, after a description of the study site and data availability in section 2.1, the proposed methods are presented in section 2.2. The results and discussion are presented in section 3 and the main conclusions are presented in section 4.

## 2. Methods and Data

### 2.1. Research Design

First, a field trip was conducted to identify the interpretation key of rice, vegetable, forest, and other crops for Sentinel-2 imagery. Using the Maximums Likelihood method was employed to classify plants based on the interpretation key, then filtering out the noise using the Majority method. The backscattering coefficient at VH of Sentinel-1 images is related to the growth of rice height. The slope of a straight line shows the variable relationship between the change in the VH backscattering value which represents the change in rice height ($\Delta y$) and the change in rice growth stages ($\Delta x$) which is determined in each image capture cycle. Finally, we make use of the planting schedule and the series of image bands of slope values to analyze the growth stage of rice. Only Sentinel-1 pixels within the boundaries of the rice growing areas identified from the Sentinel-2 imagery are used for rice maturity analysis. Each crop has a different coefficient of water use and each growth stage of the crop requires different water usage.

### 2.2. Data

The Sentinel-2 optical imagery data at 1C was collected from the European Space Agency (ESA) image database at the website https://scihub.copernicus.eu/dhus/ and the radar images of Sentinel-1 composite aperture, C band, Interferometric wide-swath mode image acquisition, 250 km, 5 × 20 m resolution at Ground Range Detected (GRD) Level 1 were collected at the following address https://search.asf.alaska.edu/. Images were collected in 2017 and 2018 for Ha Tinh province.

### 2.3. Methods

**a) Pre-Processing Satellite Images.** Beyond observing demographical data, the questionnaire was to explore the use, motivation for and effect on physical activity of wearable activity trackers as well as the technical parameters of using the device. During the survey CAWI (Computer-Assisted Web Interviewing) method was applied. The recruitment was carried out partly at university courses and partly on e-learning interface, where we placed the link directing to the questionnaire. Sentinel-2 optical imagery at level 1C has been processed with spectral radiation and orthogonal image correction. After being downloaded from ESA's database, the image was converted from level 1C to 2A which is a level where errors due to atmospheric, topographic, haze effects were removed and preliminary classification of the land cover was performed with sen2cor tool (http://step.esa.int/main/third-party-plugins-2/sen2cor). 2A-level Sentinel-2 products were resampled to have a uniform resolution for image bands. The study area of Ha Tinh province was created as a subset and the reference system was converted to the EPSG: 3405 reference system of Vietnam using SNAP Desktop, an open-source code software provided by ESA.

Sentinel-1 Level-1 IW GRD images were detected, multi-looked and projected to the ground range using an Earth ellipsoid model. After being downloaded from the database, the image was calibrated, speckle filtered and corrected for the influence of the terrain (Range-Doppler Terrain Correction). The study area of Ha Tinh province was created as a subset and the reference system was converted to the EPSG: 3405 reference system of Vietnam using SNAP Desktop software.

**b) Interpretation of Free Sentinel-2 Optical Satellite Images for Mapping the Status of Agricultural Crop Distribution.** Sentinel-2 images were interpreted by the Maximus Likelihood method, a method of classification with the inspection. The input variable for this method is a key list that interprets objects such as rice, vegetable, forest and other crops (Table 1). To develop the interpretation keys, we conducted a field trip to sample the objects to be classified. ENVI software is used to run the classification algorithms. Figure 1 is the notification window showing the results of verifying the object separability in image interpretation keys in Ha Tinh province in 2018. Classification results will be noise-filtered by the Majority method.

Sentinel-2 images taken in Ha Tinh province are significantly affected by the cloud. The Sen2Three tool is an extension of SNAP Desktop, using a series of Sentinel-2 images to eliminate cloudy pixels and replace them with clearer pixels.

**Table 1.** Interpretation key of rice, vegetable, forest and other crops on Sentinel-2 imagery and in the field

| No. | Object | Field sample | Sample of Sentinel-2 images with color combination bands 3-4-8 |
|---|---|---|---|
| 1 | Rice | 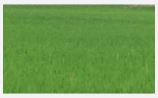 |  |
| 2 | Vegetable |   |   |
| 3 | Forest |  | 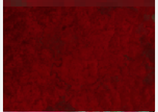 |
| 4 | Other crops |  | 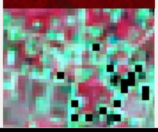 |

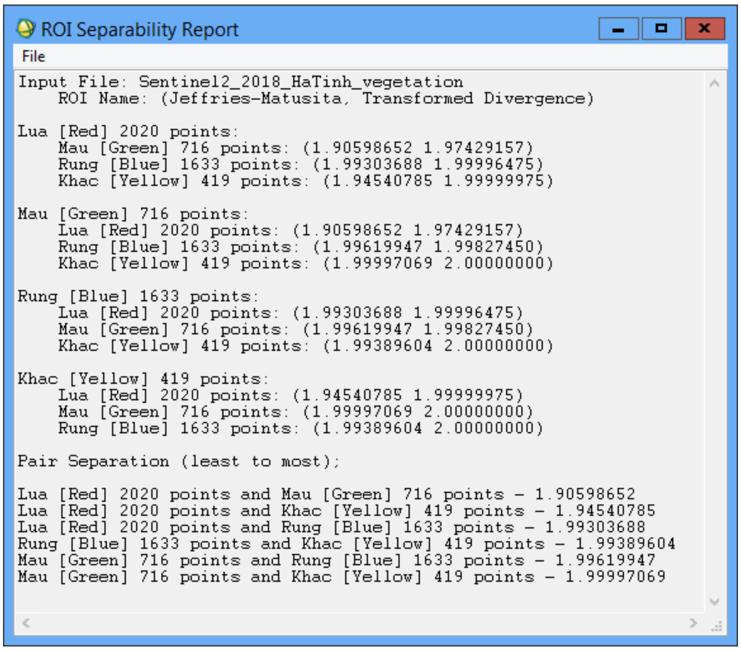

ROI Separability Report

File

```
Input File: Sentinel2_2018_HaTinh_vegetation
    ROI Name: (Jeffries-Matusita, Transformed Divergence)

Lua [Red] 2020 points:
    Mau [Green] 716 points: (1.90598652 1.97429157)
    Rung [Blue] 1633 points: (1.99303688 1.99996475)
    Khac [Yellow] 419 points: (1.94540785 1.99999975)

Mau [Green] 716 points:
    Lua [Red] 2020 points: (1.90598652 1.97429157)
    Rung [Blue] 1633 points: (1.99619947 1.99827450)
    Khac [Yellow] 419 points: (1.99997069 2.00000000)

Rung [Blue] 1633 points:
    Lua [Red] 2020 points: (1.99303688 1.99996475)
    Mau [Green] 716 points: (1.99619947 1.99827450)
    Khac [Yellow] 419 points: (1.99389604 2.00000000)

Khac [Yellow] 419 points:
    Lua [Red] 2020 points: (1.94540785 1.99999975)
    Mau [Green] 716 points: (1.99997069 2.00000000)
    Rung [Blue] 1633 points: (1.99389604 2.00000000)

Pair Separation (least to most);

Lua [Red] 2020 points and Mau [Green] 716 points - 1.90598652
Lua [Red] 2020 points and Khac [Yellow] 419 points - 1.94540785
Lua [Red] 2020 points and Rung [Blue] 1633 points - 1.99303688
Rung [Blue] 1633 points and Khac [Yellow] 419 points - 1.99389604
Mau [Green] 716 points and Rung [Blue] 1633 points - 1.99619947
Mau [Green] 716 points and Khac [Yellow] 419 points - 1.99997069
```

**Fig. 1.** The sample verifying the object separability in the 2018 image interpretation key – Interpretation of Sentinel-1 free radar satellite imagery to determine rice maturity

Sentinel-1 images provide two backscattering values, VV and VH. In this study, we use VH backscattering, which is sensitive to the crop height. VH backscatter values of radar images have different values as they are affected by different rice varieties, rice yield of each region, the topography of rice cultivating areas and the effect of speckled noise. Therefore, it is not feasible to track the set of VH values in a rice crop to identify the rice patterns. Considering a rice crop, taking the X-axis as the time of capturing the image and the Y-axis as the VH backscattering values of the pictures taken, the first point is at the starting time of sowing/transplanting and the endpoints are image capturing moments later. Thus, it is possible to define a series of straight lines with the equation $y = ax + b$. Using simple linear regression, we can determine coefficients a and b.

Assume we have n image capturing cycles from cycle 0 to cycle n-1.

Combining cycle 0 with cycle 1, we have a line $y_1 = a_1x+b_1$

Combining cycle 0 with cycle 2, we have a line $y_2 = a_2x+b_2$

Combining cycle 0 with cycle n-1, we have a line $y_{n-1} = a_{n-1}x+b_{n-1}$

The coefficient represents the variable relationship between the change in VH backscattering value that describes the change in rice height ($\Delta y$) and the change in growth time of rice ($\Delta x$). For each pixel, there is a sequence of values $a_1, a_2, \ldots, a_{n-1}$. The values of these coefficients are recorded to the image bands $Slope_1, Slope_2, \ldots, Slope_{n-1}$, respectively.

Combining the RGB color scheme between these Slope image bands, users will see the rice's change in height, thereby are able to interpolate the growth stage of the rice plant. The accuracy of this method is limited and the author group is working on improving its accuracy gradually.

Evaluating the results of interpreting Sentinel-2 images to map current agricultural crop distribution status

The method of evaluating the results of image interpretation uses error matrix and is implemented on ENVI image processing software. The two methods used are the Overall Accuracy (OA) method (1) and the Kappa Coefficient (Kappa Coefficient) method (2).

The OA is determined using the following formula:

$$OA\ (\%) = 100 * \frac{The\ number\ of\ pixels\ that\ were\ correctly\ classified}{Total\ number\ of\ pixels\ in\ the\ classification\ sample} \quad (1)$$

The Kappa coefficient is determined using the following formula:

$$K = \frac{n\sum_{i=1}^{r} x_{ii} - \sum_{i=1}^{r}(x_{i+} * x_{+i})}{n^2 - \sum_{i=1}^{r}(x_{i+} * x_{+i})} \quad (2)$$

In which:
n is the total number of pixels,
$x_{ii}$ is the pixel on the diagonal of the matrix (correctly classified pixels),
$x_{i+}$ is the total number of pixels in rows,
$x_{+i}$ is the total number of pixels in the columns.

## 3. Results and discussion

### 3.1. Results of Mapping the Distribution of Crops (Rice, Vegetables) Based on Sentinel-2 Images

Sentinel-2 image data collected in Ha Tinh province on March 5, 2018 (T48QWF) and May 16, 2018 (T48QWF, T48QXF) were used to map crop distribution using the Maximums Likelihood (Figure 2). The area of rice and vegetable crops was interpreted from the Sentinel-2 imagery in 2018 comparing to the crop area statistics shown in Table 2.

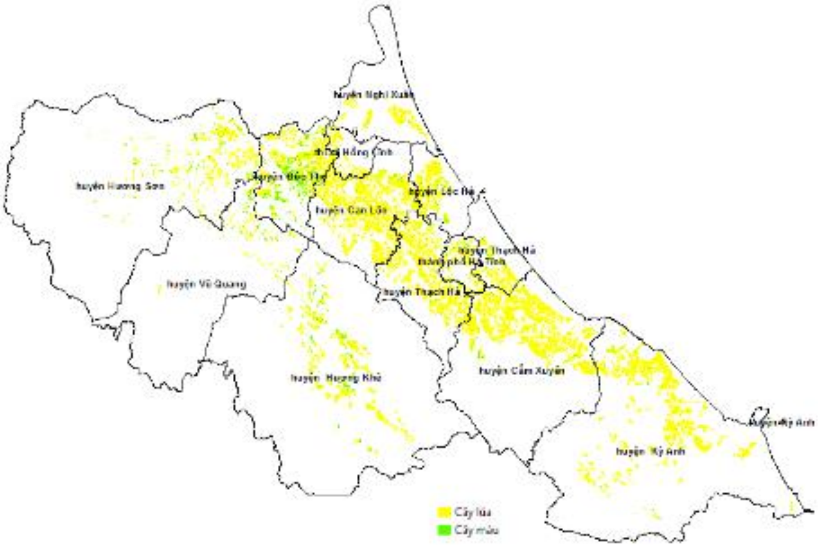


**Fig. 2.** 2018 rice and vegetable crops distribution map layer (Yellow = rice, green = vegetables)

**Table 2.** Comparison of the interpretation results of rice and vegetable cultivating areas with referenced crop areas

| Year | Interpretation Object | Area interpreted with Sentinel-2 imagery (hectares) | Referenced crop areas from Ha Tinh province (hectares) |
|---|---|---|---|
| 2018 | Rice | 64,014 | 59,143 |
| | Vegetables | 10,049 | 14,504 |

Verifying that the results of 2018 Sentinel-2 image interpretation has a Kappa coefficient of 0.89 and an OA of 92.42 %.

### 3.2. Results of Rice Crop Progression in Sentinel-1 Imagery

In order to verify the results of determining the rice maturity, Cam Hoa commune, Cam Xuyen district and Thach Hoi commune, Thach Ha district, Ha Tinh province are examined. An image series captured the winter-spring rice crop in 2018 includes 13 Sentinel-1 image cycles on January 14, January 26, February 7, February 19, March 3, March 15, March 27, April 8, April 20, May 2, May 14, May 26, and June 7, 2018, corresponding to the stages of growth and development of rice from February 6 to June 4, 2018. 12 image bands $Slope_1$, $Slope_2$,... to $Slope_{12}$ are produced. In Figure 3, the Product Explorer tab contains 12 images, the main screen opens 12 images simultaneously from $Slope_1$, $Slope_2$, ... to $Slope_{12}$, which makes it easy to see that the growth of rice changes gradually over time. Table 3 is a summary of results from the local planting calendar, rice-growing stages and color combination of image bands in Figure 3.

**Table 3.** Tables may span across both columns

| No. | Sentinel-1 image time (2018) | Number of days | Growth and development stage | Slope band |
|---|---|---|---|---|
| 1 | 14/1-7/2 | 0 | Tilting the soil and wetting the field | |
| 2 | 26/1-19/2 | 12 | Wetting the field until sowing | 1, 2, 3 |
| 3 | 7/2-3/3 | 24 | Sowing to tillering | 2, 3, 4 |
| 4 | 19/2-15/3 | 36 | Tillering | 3, 4, 5 |
| 5 | 3/3-27/3 | 48 | Tillering to leaf stem development | 4, 5, 6 |
| 6 | 15/3-8/4 | 60 | Leaf stem development | 5, 6, 7 |
| 7 | 27/3-20/4 | 72 | Leaf stem development and panicle formation | 6, 7, 8 |
| 8 | 8/4-2/5 | 84 | Panicle formation | 7, 8, 9 |
| 9 | 20/4-14/5 | 96 | Flowering | 8, 9, 10 |
| 10 | 2/5-26/5 | 108 | Flowering to ripening | 9, 10, 11 |
| 11 | 14/5-7/6 | 120 | Ripening to harvesting | 10, 11, 12 |
| 12 | 7/6 | 120 | Completed harvest | 12 |

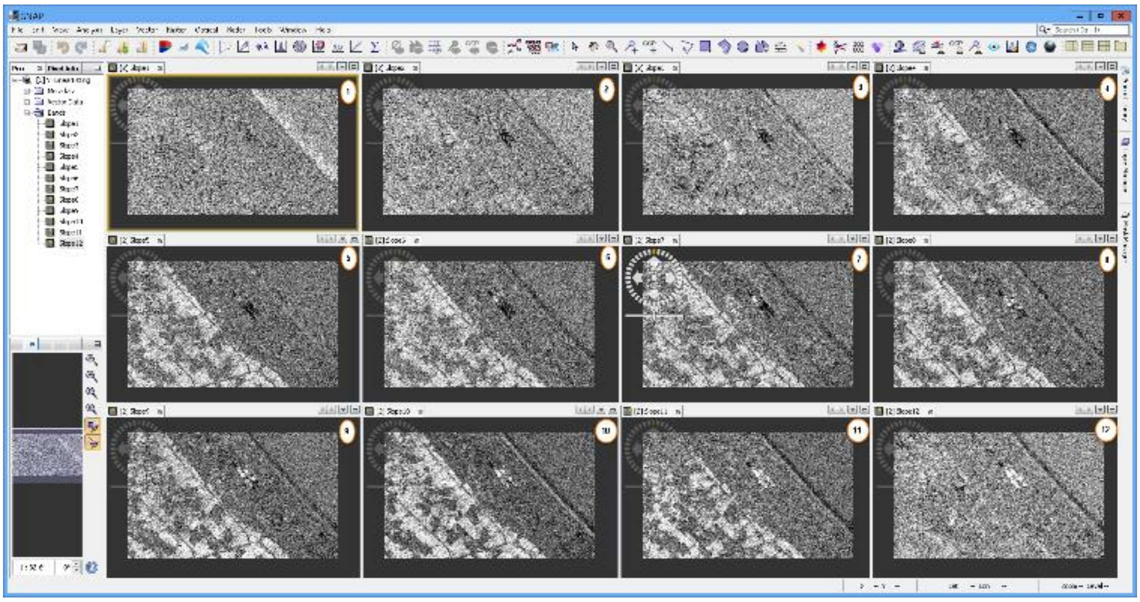

**Fig. 3.** Rice growth images through 12 Slope bands

To see the changes more clearly, the colors for three that represents the times of rice growth and development stages. Specifically, $Slope_1$ corresponds to Red, $Slope_2$ corresponds to Green, and $Slope_3$ corresponds to Blue.

Figure 4 shows the result of the color combination of $Slope_1$, $Slope_2$ and $Slope_3$ image bands from January 14 to February 19, 2018. This was the time for tilting the soil and bringing water into the rice field. Area 1 has rice on the field and rice has not appeared on area 2 yet.

Figure 5 demonstrates the result of the color combination of $Slope_2$, $Slope_3$ and $Slope_4$ image bands from February 7 to March 3, 2018. This was the time when the rice crop is still low compared to the water level in the field. Area 1 has rice in the field while area 2 appears purple which is the watercolor brought into the field with sowing/transplanting in the field.

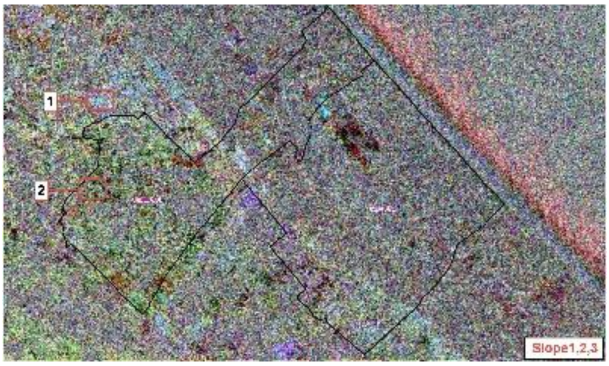


**Fig. 4.** Color combination of $Slope_1$, $Slope_2$ and $Slope_3$ image bands

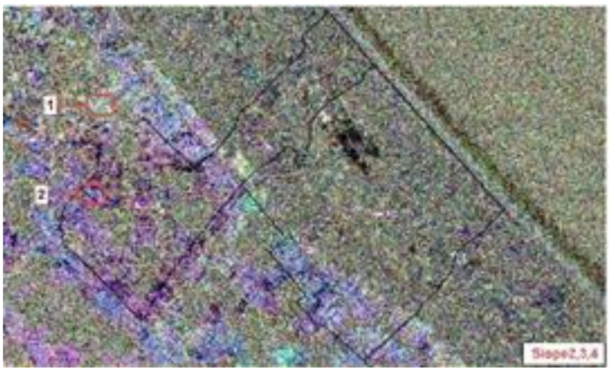


**Fig .5.** Color combination of $Slope_2$, $Slope_3$ and $Slope_4$ image bands

Figure 6 shows the results of the color combination of $Slope_3$, $Slope_4$ and $Slope_5$ image bands from February 19 to March 15, 2018. This was the time of rice growing in height, area 1's rice has moved to a new stage, area 2 has clearly recognizable rice in the field – the stage of sowing/transplanting to tillering.

Figure 10 exhibits the result of the color combination of $Slope_7$, $Slope_8$ and $Slope_9$ image bands from April 8 to May 2, 2018. At this time, the rice is tall and is in a good development stage.

Figure 11 presents the result of the color combination of $Slope_8$, $Slope_9$ and $Slope_{10}$ image bands from April 20 to May 14, 2018. Across the study area, the combined color values are quite homogeneous, which means that this is the period when the rice is at the best consecutive Slope moments are combined to form a map layer development-stage-flowering.

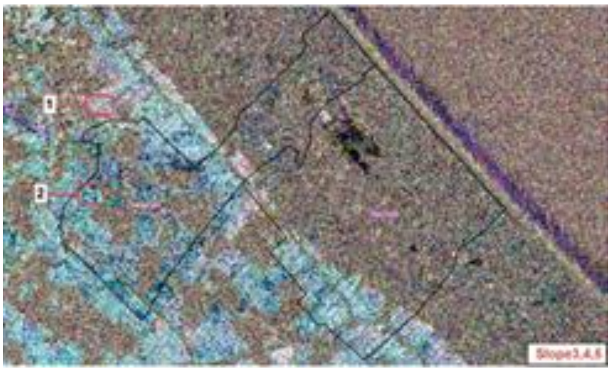


**Fig. 6.** Color combination of $Slope_3$, $Slope_4$ and $Slope_5$ image bands

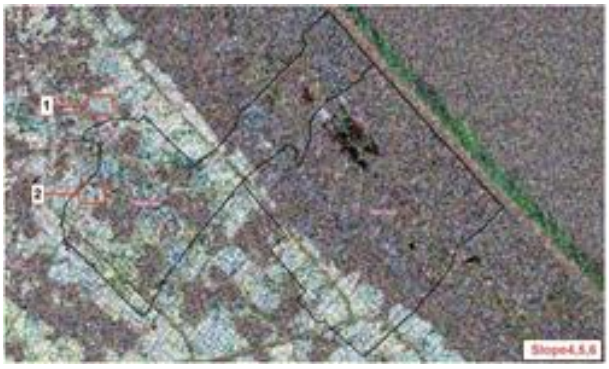


**Fig. 7.** Color combination of $Slope_4$, $Slope_5$ and $Slope_6$ image bands

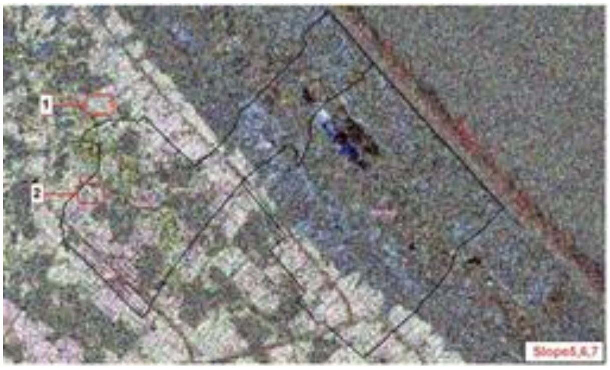


**Fig. 8.** Color combination of $Slope_5$, $Slope_6$ và $Slope_7$ image bands

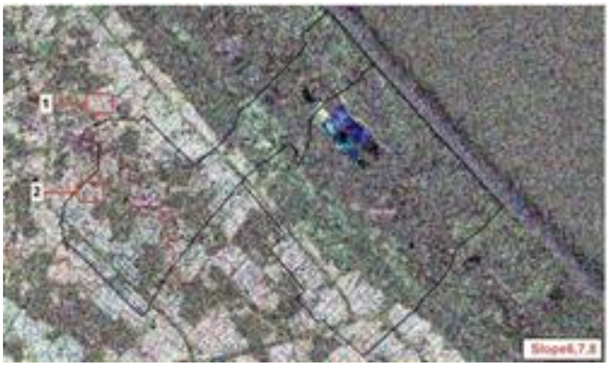


**Fig. 9.** Color combination of $Slope_6$, $Slope_7$ và $Slope_8$ image bands

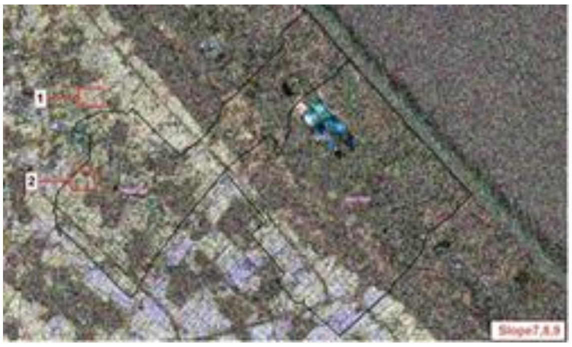

**Fig. 10.** Color combination of $Slope_7$, $Slope_8$ and $Slope_9$ image bands

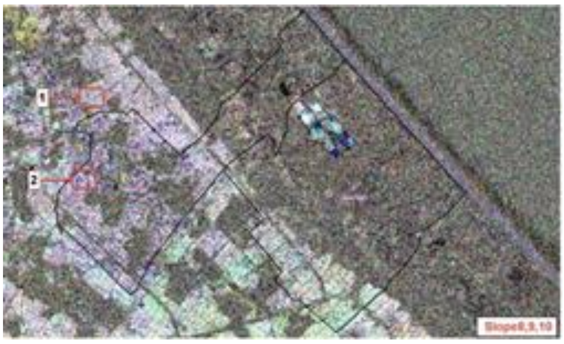

**Fig. 11.** Color combination of $Slope_8$, $Slope_9$ and $Slope_{10}$ image bands

Figure 12 shows the result of the color combination of $Slope_9$, $Slope_{10}$ and $Slope_{11}$ image bands from May 2 to May 26, 2018. Rice enters the ripening stage, the color of the combination changes significantly compared to that in Figure 11.

Figure 13 indicates the results of the color combination of $Slope_{10}$, $Slope_{11}$ and $Slope_{12}$ image bands from May 14 to June 7, 2018. Area 1 has harvested rice (dark pink), area 2 has rice at the stage of fully ripe to being harvested. The $Slope_{12}$ image band in Figure 3, taken on June 7, 2018, shows that all the rice plants have been harvested.

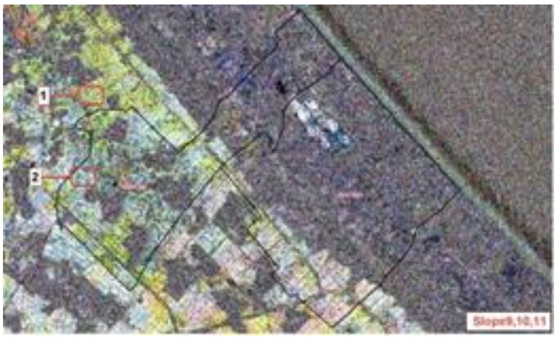

**Fig. 12.** Color combination of $Slope_9$, $Slope_{10}$ and $Slope_{11}$ image bands

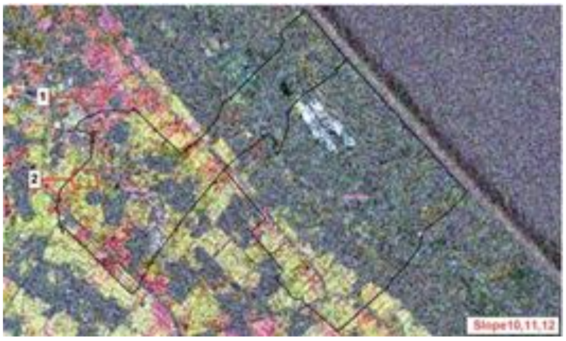

**Fig. 13.** Color combination of $Slope_{10}$, $Slope_{11}$ and $Slope_{12}$ image bands

### 3.3. Field Verification and Supplementation of Industrial Results Interpreting Satellite Images Identifying Agricultural Crops

**Field survey**

Identify sampling points (Figure 14), a GPS device was to delineate the area of crops (rice, crops) in the field, capture the entire landscape around the sampling area on the camera. (Figure 15).

**Fig. 14.** Field survey and GPS positioning of vegetable crop areas in Xuan Linh commune, Nghi Xuan district


**Fig. 15.** Locations of sampling points for agricultural crops (rice, vegetables)

**Calibrate and verify the results of image interpretation for identifying agricultural crops**

The survey locations of crops (rice, vegetables) were compiled and edited in the form of a map (.shp) where incorrect positions were corrected directly on the agricultural crop map. (.shp) from the satellite image background.

The accuracy of the map established from satellite images is computed using an error matrix. The matrix of errors is made based on comparing the results of indoor interpretation with the results of field surveys. This matrix is a square matrix with the order equals the number of layers sorted and verified. The header row of the columns (top row) shows the names of verified classes. The title column of the row (the first column) shows the names of the classified classes. The diagonal line from the top left to the bottom right of the matrix records the number of pixels or classified objects that coincide with the actual verification (exact classification). The remaining cells of the matrix record the number of pixels or objects with the following characteristics: according to the classification results, they belong to the class recorded on the column, but in fact they are verified to belong to the class recorded in the header of the row. They show the classification error and are divided into two types: errors by omission and errors by redundant inclusion.

The total classification error is calculated by dividing the total number of correctly classified pixels (i.e the total diagonal value of the matrix) by the total of classified and verified pixels. The error for each layer is calculated by dividing the total pixels of that layer with the total pixels by row or column. The ratio of the total number of correct pixels for a layer divided by the total number of pixels in a column is called error by omitting classification. The ratio of the total number of correctly classified pixels in a layer divided by the total number of pixels classified into that group by the line is called redundancy error. Table 4 shows the evaluation by Kappa coefficient.

**Table 4.** Kappa coefficient rating

| Rating | Kappa coefficient |
|---|---|
| Very good | ≥ 0.81 |
| Good | 0.80 – 0.61 |
| Average | 0.60 – 0.41 |
| Low | 0.40 – 0.21 |
| Bad | 0.20 – 0.0 |
| Very bad | < 0.0 |

**3.4. Survey and Verify the Results of Image Interpretation for Identifying the Stage of Rice Growth**

To verify the results of Sentinel-1 image interpretation to monitor the growth and development of rice (rice stage), we serveyed in the Cam Hoa commune, Cam Xuyen district and Thach Hoi commune, Thach Ha district, Ha Tinh province and evaluate the results in the study area (Figure 16): Three times in a rice crop, at critical times of the rice: sowing to tillering; panicle formation to flowering; ripening to harvesting; Measure the height of the rice plant at 20 points in the field corresponding to three important times of rice (Figures 17, 18, 19); Assess the accuracy between the height of the rice measured and the Slope value at the time of the rice stage from sowing to tillering with $R^2$ = 0.92 (Figure 20) and at the time of the rice stage from panicle formation to flowering with $R^2$ = 0.93 (Figure 21).

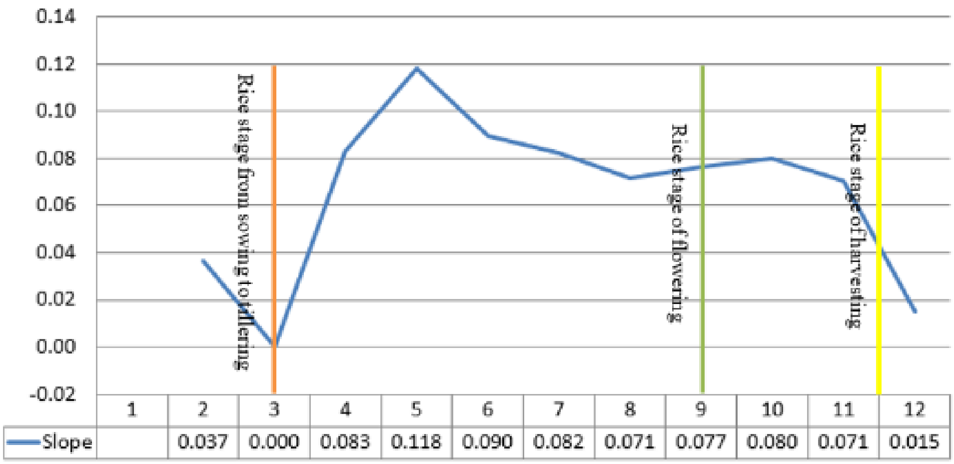


**Fig. 16.** Diagram of rice growth and development stage process interpreted from Sentinel-1 satellite images (average of 20 sample points)

**Fig. 17.** Rice stage from sowing to tillering

**Fig. 18.** Rice stage of flowering

**Fig. 19.** Rice stage of harvesting

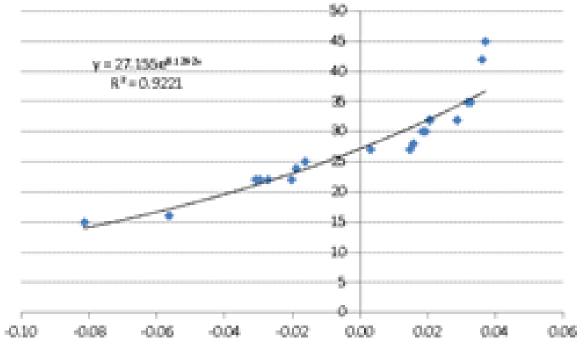


**Fig. 20.** Relations of the rice height measured with Slope value at the time of rice stage from sowing to tillering

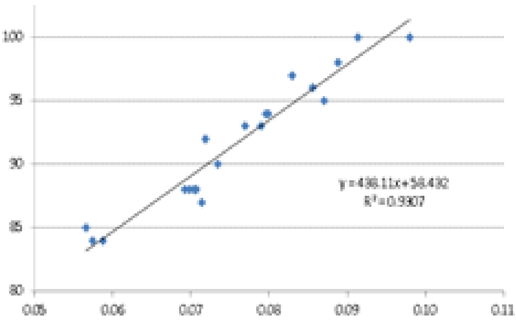


**Fig. 21.** Relations of the rice height measured with Slope value at the time the stage of flowering

## 4. Conclusion

This paper presents the methods and results of processing and interpreting Sentinel-1 and Sentinel-2 satellite images and the methods to evaluate the reliability of the interpretation results. We use the interpretation key table to interpret rice, vegetable, forest, and other plants on Sentinel-2 imagery and in the field to create a map of agricultural crops. This study also shows the relationship between the Sentinel-1 VH band and the growth of rice. From the image bands, we could calculate the slope of the line correlating between the VH backscattering value and the growth time of rice. Along with the local planting schedule, rice life cycle, and simple deduction, we could determine the rice growth stage at each time of image acquisition. We have programmed in Java to calculate the slope factor for the whole province of Ha Tinh and run it on computers with Intel Xeon processor, configuration E3-1505M v5 2.80GHz CPU, 32GB RAM memory. The time to output the result was less than 2 minutes. Therefore, a nationwide deployment will take about 2 hours. The result will be the input parameter for the irrigation management, monitoring and operating information system that is applied to Ha Tinh province for proper and effective irrigation.

## 5. Acknowledgements

This paper is one of the outputs of the research entitled "Research on application of new technologies (remote sensing, webgis, and automation) to develop information management systems for efficient use of water resources (dry season) in real-time to respond to climate change, applied to Ha Tinh province", code BDKH. 17/16-20 under Science and Technology Program to respond to climate change, natural resources and environment management during 2016 to 2020 period. The authors would like to thank the Program for funding this research.

## References

Bouvet et al., 2011 – *Bouvet, A., LeToan, T.* (2011). Use of ENVISAT/ASAR wide-swath data for timely rice fields mapping in the Mekong River Delta. *Remote Sens. Environ.* 115: 1090-1101.

Castillejo-Gonzalez et al., 2009 – *Castillejo-Gonzalez, I.L., López-Granados, F., GarcíaFerrer, A., Peña-Barragán, J.M., Jurado-Expósito, M., Sánchezde la Orden, M., González-Audicanac M.* (2015). Object and Pixelbased Analysis for Mapping Crops and their AgroEnvironmental Associated Measures Using QuikBird Imagery. *Computer, and Electronics in Agriculture.* 68: 207-215.

Cavur et al., 2015 – *Cavur, M., Kemec, S., Nabdel, L., Duzgun, H.D.* (2015). An evaluation of land use land cover (LULC) classification for urban applications with Quickbird and WorldView2 data. *Urban Remote Sensing Event (JURSE), 2015 Joint*, pp.1, 4, March 30 2015-April 1 2015.

Clauss et al., 2018 – *Clauss, K., Ottinger, M., Leinenkugel, P., Kuenzer, C.* (2018). Estimating rice production in the Mekong Delta, Vietnam, utilizing time series of Sentinel-1 SAR data. *Int. J. Appl. Earth Obs. Geoinf.* 73: 574-585.

Demirkan et al., 2017 – *Demirkan, D.C., Duzgun, H.S.* (2017). Land Use And Land Cover Classification Of Sentinel 2-A Images, Thesis.

Drusch et al., 2012 – *Drusch, M., Del Bello, U., Carlier, S., Colin, O., Fernandez, V., Gascon, F., ... Bargellini, P. (*2012). Sentinel-2: ESA's Optical High-Resolution Mission for GMES Operational Services. *Remote Sensing of Environment.* 120: 25-36.

El-Gammal et al., 2014 – *El-Gammal, M., Ali, R. R., Abaou Samra R.M.* (2014). NDVI Threshold Classification for Detecting Vegetation Cover in Damietta Governorate, Egypt. *Journal of American Science.* 10(8): 108-114.

Ndikumana et al., 2018 – *Ndikumana Emile, Dinh Ho Tong Minh, Hai Thu Dang Nguyen, Nicolas Baghdadi, Dominique Courault, Laure Hossard, Ibrahim El Moussawi* (2018). Estimation of Rice Height and Biomass Using Multitemporal SAR Sentinel-1 for Camargue, Southern France. *Remote Sens.* 10: 1394.

George et al., 2012 – *Petropoulos, G.P., Kalaitzidis, C., Prasad, Vadrevu K.* (2012). Support Vector Machines and Object-based Classification for Obtaining Land-Use/Cover Cartography from Hyperion Hyper spectral Imagery. *Computers and Geosciences.* 41: 99-107.

Hassan Bazzi et al., 2019 – *Hassan Bazzi, Nicolas Baghdadi, Mohammad El Hajj, Mehrez Zribi, Dinh Ho Tong Minh, Emile Ndikumana, Dominique Courault, Hatem Belhouchette* (2019). Mapping Paddy Rice Using Sentinel-1 SAR Time Series in Camargue, France. *Remote Sens.* 11: 887.

Immitzer et al., 2016 – *Immitzer, M., Vuolo, F., Atzberger, C.* (2016). First Experience with Sentinel-2 Data for Crop and Tree Species Classifications in Central Europe. *Remote Sens*. 8: 166.

Kaplan et al., 2018 – *Kaplan, G., Ugur, A.* (2018). Sentinel-1 and Sentinel-2 Data Fusion for Wetlands Mapping: Balikdami, Turkey. *International Archives of the Photogrammetry, Remote Sensing and Spatial Information Sciences – ISPRS Archives*. 42(3): 729-734.

Lasko et al., 2018 – *Lasko, K., Vadrevu, K.P., Tran, V.T., Justice, C.* (2018). Mapping Double and Single Crop Paddy Rice with Sentinel-1A at Varying Spatial Scales and Polarizations in Hanoi, Vietnam. *IEEE J. Sel. Top. Appl. Earth Obs. Remote Sens*. 11: 498-512.

Licheng Zhao et al., 2019 – *Licheng Zhao, Yun Shi, Bin Liu, Ciara Hovis, Yulin Duan, Zhongchao Shi* (2019). Finer Classification of Crops by Fusing UAV Images and Sentinel-2A Data. *Remote Sens*. 11: 3012.

Lopez-Sanchez et al., 2011 – *Lopez-Sanchez, J.M., Ballester-Berman, J.D., Hajnsek, I.* (2011). First Results of Rice Monitoring Practices in Spain by Means of Time Series of TerraSAR-X Dual-Pol Images. *IEEE J. Sel. Top. Appl. Earth Obs. Remote Sens*. 4: 412-422.

Cavur et al., 2019 – *Cavur, M., Duzgun, H.S., Kemec, S., Demirkan, D.C.* (2019). Land use and land cover classification of Sentinel-2A: ST Petersburg case study. *The International Archives of the Photogrammetry, Remote Sensing and Spatial Information Sciences,* Volume XLII-1/W2.

Maglione et al., 2013 – *Maglione, P., Parente, C., Vallario, A.* (2013). Using Worldview-2 Satellite Imagery To Support Geoscience Studies On Phlegraean Area. *American Journal of Geosciences*. 3(1): 1-12.

Manakos et al., 2014 – *Manakos, I., Lavender, S.* (2014). Remote sensing in support of the geo-information in Europe. *Remote Sensing and Digital Image Processing*. 18.

Manuel et al., 2019 – *Manuel Campos-Taberner, Francisco Javier García-Haro, Beatriz Martínez, Sergio Sánchez-Ruíz, María Amparo Gilabert* (2019). A Copernicus Sentinel-1 and Sentinel-2 Classification Framework for the 2020+ European Common Agricultural Policy: A Case Study in València (Spain). *Agronomy*. 9: 556.

Ndikumana et al., 2018 – *Ndikumana, E., HoTong Minh, D., Baghdadi, N., Courault, D., Hossard, L.* (2018). Deep Recurrent Neural Network for Agricultural Classification using multitemporal SAR Sentinel-1 for Camargue, France. *Remote Sens*. 10: 1217.

Neetu et al., 2019 – *Neetu, Ray, S.S.* (2019). Exploring machine learning classification algorithms for crop classification using Sentinel-2 data. *The International Archives of the Photogrammetry, Remote Sensing and Spatial Information Sciences*. Volume XLII-3/W6, ISPRS-GEOGLAM-ISRS Joint Int. Workshop on “Earth Observations for Agricultural Monitoring”, 18–20 February 2019, New Delhi, India.

Nelson et al., 2014 – *Nelson, A., Setiyono, T., Rala, A., Quicho, E., Raviz, J., Abonete, P., Maunahan, A., Garcia, C., Bhatti, H., Villano, L. et al.* (2014). Towards an Operational SAR-Based Rice Monitoring System in Asia: Examples from 13 Demonstration Sites across Asia in the RIICE Project. *Remote Sens*. 6: 10773-10812.

Nguyen et al., 2015 – *Nguyen, D., Clauss, K., Cao, S., Naeimi, V., Kuenzer, C., Wagner, W.* (2015). Mapping Rice Seasonality in the Mekong Delta with Multi-Year Envisat ASAR WSM Data. *Remote Sens*. 7: 15868-15893.

Petropoulos et al., 2007 – *Petropoulos, G.P., Knorr, W., Scholze, M. Boschetti, L. Karantounias, G.* (2007). Combining ASTER Multispectral Imagery Analysis and Support Vector Machines for Rapid and Cost-Effective Post-Fire Assessment: A Case Study from the Greek Wildland Fires of 2007. *Nat. Hazards Earth Syst. Sci*. 10: 305-317.

Qiao et al., 2012 – *Qiao, C., Luo, J., Sheng, Y., Shen, Z., Zhu, Z., Ming, D.* (2012). An Adaptive Water Extraction Method from Remote Sensing Image Based on NDWI. *Journal of the Indian Society of Remote Sensing*. 40(3): 421-433.

Radoux et al., 2016 – *Radoux, J., Chomé, G., Jacques, D.C., Waldner, F., Bellemans, N., Matton, N., Lamarche, C., D’Andrimont, R., Defourny, P.* (2016). Defourny, Sentinel-2’s potential for subpixel landscape feature detection. *Remote Sensing*. 8(6).

Raziye Hale et al., 2016 – *Raziye Hale, Elif Nebiye* (2016). Assessment of classification accuracies of Sentinel-2 and Landsat-8 data for land cover/use mapping. *The International Archives of the Photogrammetry, Remote Sensing and Spatial Information Sciences*. Volume XLI-B8, 2016 XXIII ISPRS Congress, 12–19 July, Prague, Czech Republic.

Stavros Patsalidis et al., 2019 – *Stavros Patsalidis, Athos Agapiou, Diofantos G. Hadjimitsis* (2019). Random forest classification analysis of Sentinel-2 and Landsat-8 images over semi-arid environment in the Eastern Mediterranean. AGILE 2019 – Limassol, June 17-20.

Tian-Xiang Zhang et al., 2019 – *Tian-Xiang Zhang, Jin-Ya Su, Cun-Jia Liu, Wen-Hua Chen* (2019). Potential Bands of Sentinel-2A Satellite for Classification Problems in Precision Agriculture, 2019, Springer. International Journal of Automation and Computing.

Wang et al., 2005 – *Wang, L.-F.,Kong, J.A., Ding, K.H., Le Toan, T., Ribbes, F., Floury, N.* (2005). Electromagnetic scattering model for rice canopy based on monte carlo simulation. *Prog. Electromagn. Res*. 52: 153-171.